

EXAMINING BIOMARKERS IN SEDIMENTARY DEPOSITS OF OCEAN ANOXIC EVENT 2

By

LEAH VICTORIA ORTEGA

A Thesis Submitted to The Honors College

In Partial Fulfillment of the Bachelors degree

With Honors in

Biochemistry

THE UNIVERSITY OF ARIZONA

M A Y 2 0 1 9

Approved by:

Dr. Jessica Tierney

Department of Geoscience

Abstract:

Oceanic Anoxic Event 2 occurred near the Cenomanian-Turonian boundary ca. 93.5 million years ago. Global warming and an enhanced hydrological cycle fueled ocean productivity, resulting in worldwide deposition of organic carbon-rich black shales. Some of the best exposures of OAE-2 are in the Apennine mountains in Italy. The purpose of this project was to investigate whether black cherts from these localities have better preservation of biomarkers that record climate conditions during the event than black shales. We examined seven samples that were collected from two different outcrops: one in Furlo, Italy and another at the Contessa quarry, about 30 miles away. From the data, it was found that the preserved fatty acids were likely from marine biomass rather than terrestrial life. These fatty acids also revealed that the cherts were better preservers than shales for the fatty acids. By evaluating the GDGTs, it was found that the average sea surface temperature was 41.2°C.

Introduction:

Ocean Anoxic Event 2 (OAE-2), also referred to as the Bonarelli Event, occurred 93.5 million years ago in the mid-Cretaceous era close to the Cenomanian-Turonian boundary (Schlanger and Jenkyns, 1976). During this event, one of the several Mesozoic intervals of widespread ocean anoxia and euxinia occurred which produced large amounts of organic-rich black shale. This black shale is thought to be caused by the enhancement of organic carbon burial in marine



Image 1. OAE-2 in the Furlo section of the Apennine mountains. (Photo by Dr. Jessica Tierney).

sediments during the event. A few of the best exposures of the OAE-2 is found in the Apennine mountains in Italy (*Image 1*).

The cause of the oceanic events during the Cretaceous era is still widely under debate, however evidence and models have supported enhanced productivity that caused a flux in organic carbon in sediments as the source for the oxygen depletion during this time. Mechanisms for this productivity includes ocean upwelling, the enhancement of surface waters mixing, and the increase of nutrients coming from the continent and into the water (Nederbragt, et al., 2004). Certain greenhouse conditions (i.e. hydrological cycle and increased weathering) are linked to this increase in productivity. OAE-2 is marked by a positive excursion in stable carbon isotopes ($\delta^{13}\text{C}$) records which indicates the high burial rates of organic carbon in deep marine sediment. Major paleoenvironmental changes such as high sea-levels, high atmospheric temperatures, and increasing sea-surface temperatures have also been associated with the OAE-2 (Westermann, 2014). Therefore, part of the purpose for this study is to determine if the collected rocks within this area are found to be efficient preservers that can be used in further studies concerning the climate changes during this event.

This project analyzed rock samples collected from two locations where OAE-2 is exposed: Furlo, Italy and the Contessa quarry, which are approximately 30 miles apart. As a point of reference, the Furlo section is located 25 km southeast of Urbino within the homonymous gorge, and the Contessa quarry is in the Vispi active quarry approximately 2 km from Gubbio (Gambacorta, et al., 2016). Three types of sediment samples were collected: chert, chert/shale, and shale. The biomarkers in these rock samples were then analyzed to assess the preservation and the maturity of the organic material, as well as sea surface temperatures (SSTs) during OAE-2.

SSTs can be calculated from the TEX₈₆ proxy. TEX₈₆ stands for the TetraEther index of 86 carbons, and is a ratio that expresses the degree of cyclization that best correlates with the SST. The cyclization is used to determine temperature based on the understanding that more rings in the GDGTs correlate to a higher melting point. GDGTs are two C₄₀ isoprenoid chains which go head-to-head. GDGTs' structures vary in numbers of cyclopentane and cyclohexane, and are connected by ether bonds to terminal glycerol groups. For sedimentary GDGTs, these structures are expected to have terminal hydroxyl groups, especially in ancient sediments. GDGTs are categorized as lipids produced by Archae; however, Thaumarchaeota is not the only source of these lipids but may include other methanogenic, hyperthermophilic, and mesophilic species. Since the early 1990s, it was found that the mesophilic relatives of extremophile Archae lived in marine environments. This discovery would soon open the doors to analyzing the GDGT's structure in order to evaluate the marine system (Tierney, 2014).

TEX₈₆ is an index that is based on relative degree of cyclization within the GDGTs. It has been calibrated with a database of 1095 modern surface sediments TEX₈₆ measurements, which has been collected from surface sediments that are known to involve overlying water temperatures related to historical observations (Tierney and Tingley, 2015). One of the limitations of using TEX₈₆ is preservation. GDGTs are refractory compounds; however the functional groups of the GDGTs (i.e. the ether-bound glycerol with polar heads) do degrade over time. For each GDGT isomer, the bacteria that degrades the organic compound attacks these functional groups first, but it has been found that degradation of the different isomers occur at the same rate causing no indication of bias in the TEX₈₆ proxy. In terms of maturity, it was found that TEX₈₆ is not affected by salinity or temperature under 240°C (Forster, et al., 2007;

Schouten, et al., 2004). This temperature will not be reached in a natural setting; therefore, the gradual rate of degradation of the functional groups make GDGTs highly preservable.

The purpose of this project was to investigate whether black cherts from the Italian sites have better preservation of biomarkers that recorded the climate change during the event compared to black shales. The biomarkers that were then found to be efficiently preserved were further analyzed to determine the maturity of the organic material and the sea surface temperature during the OAE-2.

Methods:

1. Preparation for ASE

Contamination on the exterior of each rock sample was removed using an electric rotary tool with abrasive tips. The abrasive tips were cleaned using DCM in between each sample. Once a rock sample was sufficiently cleared of exterior contamination, it was weighed and sealed in a whirlpak. Prior to grinding, the rock samples were rinsed three times using methanol and DCM. Samples were ground to a fine powder using a mortar and pestle (for Furlo OAE2, Furlo Chert-Shale, Furlo Shale, and Contessa OAE2) or a Shatterbox (Furlo Chert I, Furlo Chert II, and Contessa Chert). The mortar and pestle were rinsed three times using methanol and DCM at the beginning, end, and between each sample. The Shatterbox was rinsed with tap water, DI water, and methanol in between samples. Ground powder was then poured into a new whirlpak with assistance of a clean spatula and weighed.

2. ASE Extraction

The Accelerated Solvent Extraction ASE 350 was first prepared to contain a sufficient amount of 9:1 mixture of DCM:MeOH that was used to run the samples through the machine. The powdery rock samples were then placed into a clean 22 mL cell equipped with

glass filters. Within each cell, an appropriate amount of each sample was added based on its richness in sediment. These amounts ranged from approximately 3 grams to 30 grams. Precombusted diatomaceous earth (DE) was also added to the cell along with the samples. As a blank, a cell was also filled with only DE to test for contamination. The weight of the samples prior to entering the cells and post-cell preparation was recorded. The prepared cells were placed on the ASE while clean vials with foil caps were placed inside the machine to collect the Total Lipid Extracts (TLE). Once the TLEs were collected into the 60 mL vials, the vials were blown down. Once blown down, the TLE were transported into clean 4 mL, and 100 μ L of internal standard and GDGT standard was added to each sample.

3. *Copper Column*

The elemental sulfur derived from the microbial reduction of sulfate was removed using activated copper columns. Each sample was run through this column and collected into clean 4 mL vials.

4. *Column chromatography*

4.1 *NH₂ Column*

The TLE were separated into neutral and acid fractions using a LC-NH₂ gel column and DCM:IPA (2:1), 4% acetic acid, methanol respectively to elute a neutral, acid, and polar fraction, respectively. The fractions were blown down under N₂ gas. The acid fraction was derivatized as described below, while the neutral fraction was put through a second silica gel column.

4.2 *Activated Si Gel*

The neutral fractions of each sample were processed through an activated silica gel column in order to separate the alkanes (eluent: hexane), aromatic compounds (eluent:hexane:DCM 70:30), and the GDGTs (eluent: methanol) in each sample.

5. *FAME Extraction*

5.1 *Methylation*

This process was used to “derivatize” the acid fraction before it was analyzed by the Gas Chromatography-Flame Ionization Detector (GC-FID). In this process, the acid functioning group is replaced with a methyl group to form a fatty acid methyl ester (FAME). Acetyl chloride solution was added to cold GC grade methanol at a ratio of 5:95 (Acetyl chloride:Methanol) to produce an acidified solution. 300 μ L of toluene was added to each of the vials containing the acid fractions. In addition, the phthalic acid isotope standard was made by blowing down 1 mL of phthalic acid solution in a 4 mL vial and dissolving the solution using 300 μ L of toluene. 1 mL of acidified methanol was added to each sample, and the headspace of the vial was filled with nitrogen gas and the vial was capped tightly. Each sample was then placed on a heating block set at a temperature of 50°C and left overnight to complete the reaction. At the start of the next morning, the heating block was turned off and the samples were left to cool on the block. The final samples thus included the FAMEs and a PAME, which was the phthalic acid isotope standard turned into a phthalic acid methyl ester.

5.2 *Liquid-liquid extraction*

Once the samples were cooled after methylation, the organic phase was separated from water (the by-product of the methylation reaction) by adding sodium chloride solution to each vial along with 0.5 to 1 mL of hexane. The vials were vortexed for ten seconds and then allowed to stand in order to form the two layers. The top layer was removed using a glass

pipette and transferred to a pre-labelled 4 mL vial. This process was repeated twice for each sample, and the vials were blown down under nitrogen gas. When performing this process for the PAME, the process was the same except that DCM was used instead of hexane. This led to the bottom layer being removed and placed into a new label rather than the top. Before moving onto the last step of this process, the PAME was directly transferred to the 2 mL vial using DCM. The FAMEs were subject to one more silica gel column for purification.

5.3 Clean-Up Column

Prior to the final clean-up column, each sample was checked for noticeable salt and water. If there was a large amount located in the sample vials, those samples went through an extra step, the Sodium Sulfate columns, which can be viewed in Methods #6. Once all samples were declared “dried” and without salt, the final clean-up column occurred. Each FAME sample was purified by elution through 5% deactivated silica gel with DCM. Samples were blown down with nitrogen gas and transferred into 2 mL vials using 500 μ L of DCM.

6. Sodium Sulfate Columns

In order to remove the water and salt from the samples prior to running them on the machine, the sodium sulfate column was used. This column was not used for all samples, but only on those that showed signs of possible salt and/or water contamination after being blown down. This was the case when evaluating the FAME fractions for Furlo Chert-Shale and the Furlo Chert I. A column was set up using a sterile glass pipette and placing it in a column holder. A small ball of glass wool was placed at the base of the pipette, which allowed for the pipette to be filled half way with sodium sulfate. This column was pre-cleaned with DCM by filling the column three times with the solution and letting it drain into a waste beaker. The sample was then dissolved and loaded by using DCM. The sample vial

and column were rinsed three times using the same solution. This was then eluted into a vial labeled the same as the vial the FAME sample was originally held in. Once the column was complete, a column pusher was used to remove the last amount of liquid in the column and the samples were blown down using the Glas-Col FlexiVap Work Station with nitrogen gas.

7. *Quantitative and Qualitative Analysis*

8.1 *HPLC-MS:*

The MeOH fraction of each sample was filtered and dissolved into 40 μL of HEX:IPA (99:1), and then analyzed for GDGTs using an Agilent 1260 Infinity-MS with a 6120 single Quadrupole LC-MS equipped with 2 BEH-HILIC columns (2.1 \times 150 mm, 1.7 μm ; Waters). The machine was set to have a flow of 0.2 mL per min at a pressure of 500 bar. At start time, the solvent used was at 82% HEX and 18% HEX:IPA for 49 minutes. At minute 49, the solvent changed to 65% HEX and 35% HEX:IPA, and lasted for one minute. At 50 minutes, only HEX:IPA was released in the flow for twelve minutes. The final flow included again 82% HEX and 18% HEX:IPA, and ended at minute 75. Once all the samples were ran, peaks were calculated using the ORIGAmI MATLAB package. GDGTs were quantified by comparing these peaks to the C₄₆ internal standard. TEX₈₆ was then used to calculate the sea surface temperature (SST) using the following equation:
$$\frac{[GDGT-2+GDGT-3+cren']}{[GDGT-1+GDGT-2+GDGT-3+cren']}$$

(Fleming & Tierney, 2016)

8.2 *GC-FID: Gas Chromatography-Flame Ionization Detector*

The alkane and acid fractions were redissolved in 100 μL to 1000 μL of hexane and alkanes and FAMES were quantified using a Thermo Scientific Trace1310 with a programmable temperature vaporization (PTV) inlet equipped with a 30 m DB-5 column (0.32 mm diameter with a 0.25-micron stationary phase) and helium as the carrier gas. The

GC program for the alkanes was set at an initial temperature of 60°C and held for two minutes. This temperature increased at a rate of 20°C/min to 170°C without any hold time. The final temperature of 325°C was reached at a rate of 8°C/min and held there for thirteen minutes. The GC program for the FAMES also was set at an initial temperature of 60°C and held for two minutes. At a rate of 20°C /min, the temperature increases to 190°C with no hold time. The final temperature of 325°C was reached at a rate of 8°C/min and held for 14.6 minutes until the end of the running time. Once all the samples were ran, we processed the data using the ORIGAmI MATLAB package in order to find the carbon preference index value and the abundance of each carbon length (Fleming & Tierney, 2016). The carbon preference index uses the following equation for calculations: $CPI =$

$$0.5 \left(\frac{\text{Sum}(\text{Even Carbon Chains})}{\text{Sum}(\text{Odd Carbon Chains})} \right).$$

Results:

The recovery of biomarkers was possible in all samples except for the Contessa Chert sample. Therefore, this rock sample was excluded from subsequent analyses.

Fatty Acids

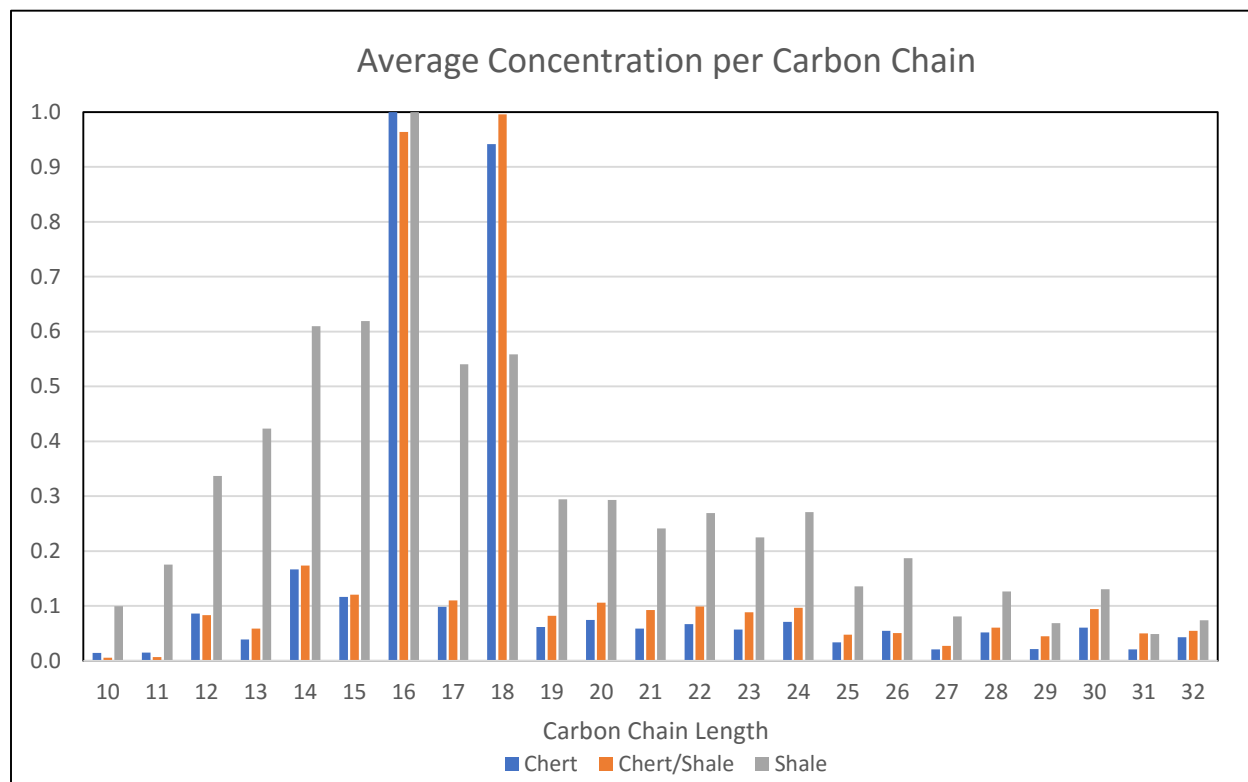


Figure 1 The average concentration value within the Chert, Chert/Shale, and Shale grouping. Concentrations were normalized to the largest peak of each grouping. Cherts and chert/shales show more distinct even-over-odd preference.

After running the FAME fractions through the GC-FID, the length of the fatty acids was identified. As can be seen in *Figure 1*, the carbon chains ranged from a value of 10-carbon chains to 30-carbon chains. With further examination, it is apparent that there is a preference for shorter carbon chains (i.e. the range of 10 to 24 carbons), especially at a chain length of 16 to 18 carbons. There was no evidence of contamination to be found within these samples during evaluation to skew the data towards 16- and 18-carbon chains.

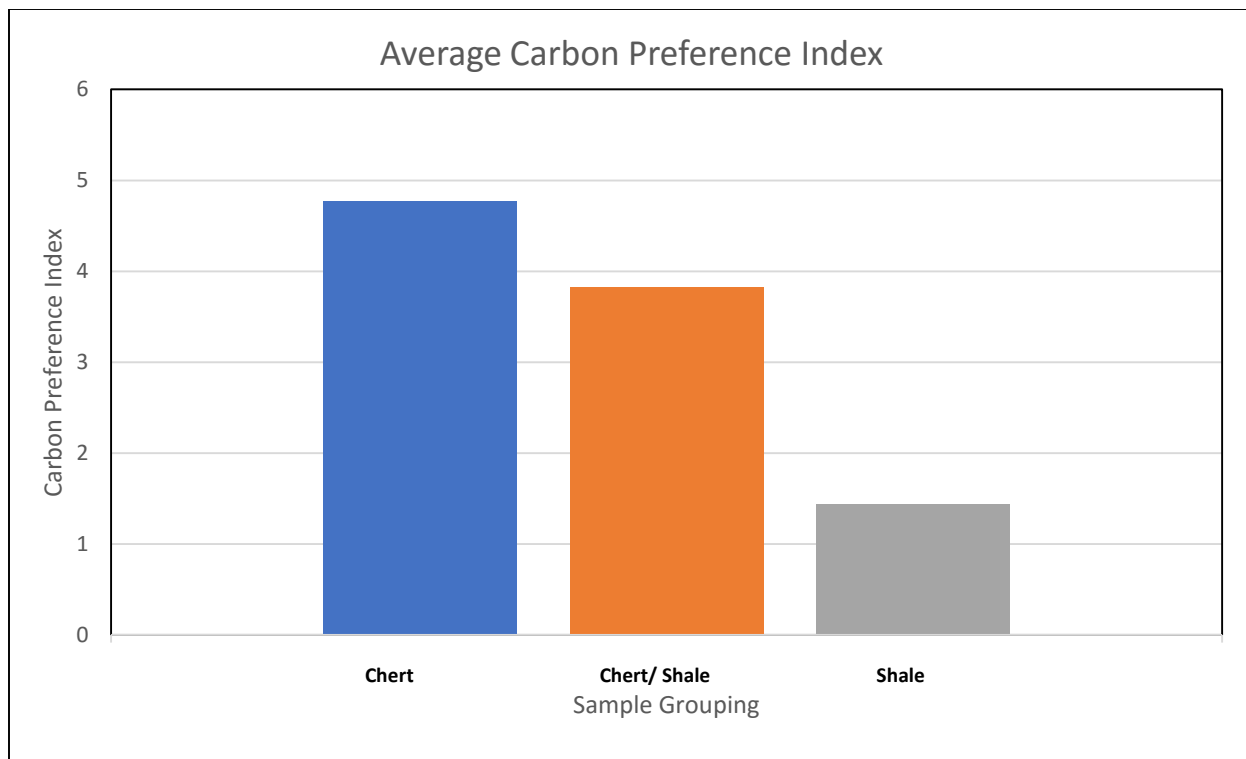


Figure 2 The average carbon preference index value within the Chert, Chert/Shale, and Shale grouping. The black cherts have the highest CPI indicating better preservation of fatty acids.

In addition to identifying the length of the fatty acids preserved in the rock samples, the data also provides insight into the quality of the preservation within each sediment. After running the FAME fractions through the GC-FID, the carbon preference index (CPI) was calculated and is presented in *Figure 2*. CPI is a calculation based off the peaks of the fatty acids and refers to the ratio of even carbon chains to odd carbon chains. Prior to finding the carbon reference index, the rocks were categorized into groups based on their sediment types: cherts, chert/shale, and shale. *Figure 2* reveals that the highest carbon preference value is found in the black chert samples, followed by the chert-shale intermediate samples, with the shales having the lowest index.

Glycerol Dialkyl Glycerol Tetraethers (GDGTs)

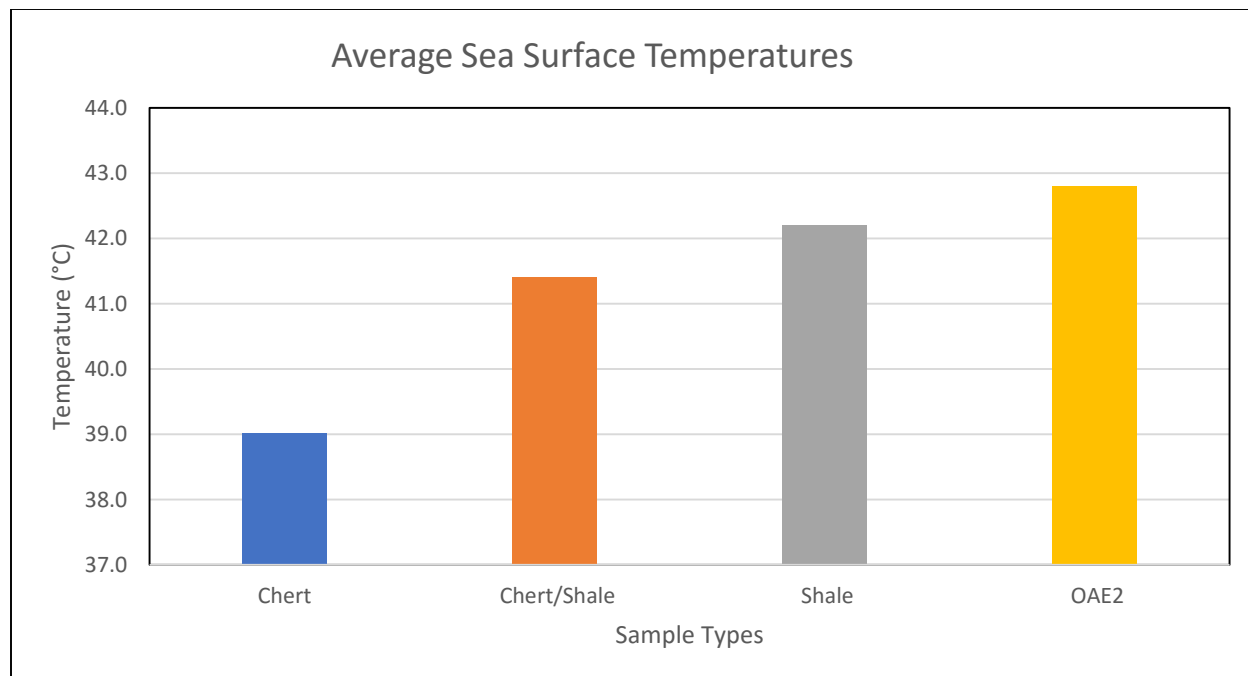


Figure 3 Calculated SSTs for the Furlo by lithology. We were able to recover GDGTs from the Furlo sections, but not the Contessa section.

From the glycerol dialkyl glycerol tetraethers (GDGTs) that were collected from these rock sediments using the HPLC-MS, a sea surface temperatures (SST) were approximated using TEX₈₆. The samples that are represented in this figure only include those collected from the Furlo section since no GDGTs were collected from the Contessa samples. Samples were grouped same as the other figures, except the OAE-2 shale, which was separated in order to investigate SSTs during the event. *Figure 3* reveals that the average temperature per group averaged from 39°C to 43°C. As shown, chert had an average SST of 39°C, chert/shale of 41.4°C, shale at 42.2°C, and OAE-2 of 42.8°C. The overall average SST was found to be 41.2°C.

Alkanes

When analyzing the alkanes through the GC-FID, it was found that the peaks for the alkanes were low abundance and co-eluted with steranes and hopanes. For this reason, the alkane data was not reviewed any further. Further study is needed, likely via GC-MS, to identify the peaks in the alkane fraction.

Discussion:

Fatty Acids

The fatty acid data show that there was a preference for shorter carbon chains (*Figure 1*), which provides insight about the producer of these fatty acids during the OAE-2. Land plants have the tendency to produce longer even-carbon number fatty acids with carbon chains amounting to 22 to 36 carbons (Eglinton & Hamilton, 1967). In contrast, marine phytoplankton produce shorter chains (16 to 18 carbons). Our samples are dominated by these shorter-chain fatty acids (*Figure 1*), which supports the idea that these preserved fatty acids derive mainly from marine life that lived during the time of this event since marine life tends to highly produce fatty acid chains of 16 and 18 carbon (Ackman, 1967).

The quality of preservation of these fatty acids was evaluated using the carbon preference index (CPI) (*Figure 2*). This ratio gives insight into the preservation because living things produce fatty acids with even carbon chains rather than odd chains. In contrast, odd chains become more dominant if the rocks are buried and heated to the point where organic matter begins to alter. If the CPI is high, it means that the fatty acids are unlikely to be altered by burial. *Figure 2* reveals that black cherts were better preservers of fatty acids compared to the shales. One possible reason for shale's inability to withhold its strength under times of friction. In a study, it was observed that the shale's strength linearly depleted with increasing clay and organic matter (Kohli and Zoback, 2013). Other studies have shown that shale's structure is also dependent on temperature and pressure. For instance, the shale's structure was found to be permanently deformed after reaching temperatures above room temperature. These deformities include the inelasticity of the sediment, making it unable to be an efficient preserver (Johnston, 2002). Cherts, on the other hand, were found to withstand higher temperatures compared to

chert. In one study, it was found that cherts toughness had a slight decline when heated to 300°C, 400°C, and 500°C with small changes to in mechanical and flaking properties. It was later discussed that, at these high temperatures, cherts may undergo microcracking and strain. Yet, the heat was also found to increase the crystal order within the rocks (Domanski and John, 1992). This entails that cherts gain a more defined structure, which makes it sturdier. Due to shale's weaken structure, the even chains that were originally preserved in the shales may have deteriorated into odd chains causing the ratio to fluctuate towards the lower CPI value represented in *Figure 2*, while chert's physical properties make them more sturdy when heat increases causing them to preserve the fatty acids better within its structure.

Glycerol Dialkyl Glycerol Tetraethers (GDGTs)

Using the GDGT TEX₈₆ to calculate the sea surface temperature, the overall average SST during the OAE-2 was 41.2 °C, which is within the range of temperatures that past literature has calculated. From *Figure 3*, it is shown that the range of SSTs vary based on the type of sediment the GDGTs were collected from. As shown, chert had a SST of 39°C, chert/shale at 41.4°C, shale at 42.2°C, and OAE-2 at 42.8°C. The OAE-2 sample is a sediment that was formed during the exact time of the oceanic anoxic event, which would also be the time when carbon dioxide concentrations were very high in the atmosphere. Hence, we expect this sample to exhibit the highest SST. However, the calibration of TEX₈₆ at such high temperatures is uncertain, with an error of 5.8°C. Including the error margin, the derived temperature (41.2°C) would be in range with other works that have found the reconstructed SST to be from 32°C to 39°C (Schouten, et al., 2003; Forster, et al., 2007; van Helmond, et al., 2014). As these GDGTs were analyzed, it was found that those rocks collected from the Furlo site were the only samples able to provide GDGTs. Other studies have shown that samples from both the Furlo site and Contessa site have

had similar results when collecting data; therefore, further studies into what determines the strength of preservation of the rocks from each site should occur (Westermann, 2014).

Conclusion:

From the collected rocks, it was found that certain biomarkers, fatty acids and GDGTs, were preserved effectively and were able to be analyzed to determine characteristics of the climate during the OAE2. Using TEX₈₆, we were able to use the GDGTs preserved in the rock samples to find that the average sea surface temperature was 41.2°C. While evaluating the other biomarker, it was found that the cherts had a better quality of preservation for the fatty acids compared to the shales. Through the evaluation of the fatty acids, there was also an indication that the material preserved within these sedimentary rocks were produced by marine biomasses. In the future, we plan to further investigate the maturity of this organic material by identify the molecules preserved within these rock samples, specifically the steranes and hopanes.

Acknowledgement:

I would like to thank Patrick Murphy for his constant support and help when completing this project. I would also like to thank Dr. Jessica Tierney for her help and feedback throughout the entire process. Lastly, thank you to everyone apart of the Tierney lab for their advice and words of encouragement.

References:

1. Ackman RG. Characteristics of the Fatty Acid Composition and Biochemistry of some Fresh-Water Fish Oils and Lipids in Comparison with Marine Oils and Lipids. *Comparative Biochemistry and Physiology*. 1967; 22(3), 907-922.
2. Domanski M, Webb JA. Effect of Heat Treatment on Siliceous Rocks Used in Prehistoric Lithic Technology. *Journal of Archaeological Science*. 1992; 19(6), 601-614.
3. Eglinton G, Hamilton R. Leaf Epicuticular Waxes. *Science*. 1967; 156(3780), 1322-1335.
4. Fleming LE and Tierney JE. An automated method for the determination of the TEX86 and U37K' paleotemperature indices. *Organic geochemistry*. 2016; 92, 84-91.
5. Forster A, Schouten S, Moriya K, Wilson PA, Sinninghe Damste JS. Tropical warming and intermittent cooling during the Cenomanian/Turonian oceanic anoxic event 2: Sea surface temperature records from the equatorial Atlantic. *Paleoceanography and Paleoclimatology*. 2007; 22(1), 1-14.
6. Gambacorta G, Bersezio R, Weissert H, Erba E. Onset and demise of Cretaceous oceanic anoxic events: The coupling of surface and bottom oceanic processes in two pelagic basins of the western Tethys. *Paleoceanography*. 2016; 31(6), 625-913.
7. Kohli AH, Zoback MD. Frictional properties of shale reservoir rocks. *Journal of Geophysical Research: Solid Earth*. 2013; 118(9), 5109-5125.
8. Johnston DH. Physical properties of shale at temperature and pressure. *Geophysics*. 2002; 52(10), 1391-1401.
9. Neberbragt AJ, Thurow J, Vonhof H, Brumsack HJ. Modelling oceanic carbon and phosphorus fluxes: implications for the cause of the late Cenomanian Oceanic Anoxic Event (OAE2). *Journal of the Geological Society*. 2004; 161(4), 721-728.

10. Schlanger SO, Jenkyns HC. Cretaceous Oceanic Anoxic Events: Causes and Consequences. *Netherlands Journal of Geosciences Foundation*. 1976; 55(3-4), 179-184.
11. Schouten S, Hopmans EC, Forster A, van Breugel Y, Kuypers MM, Sinninghe Damste JS. Extremely high sea-surface temperatures at low latitudes during the middle Cretaceous as revealed by archaeal membrane lipids. *Geology*. 2003; 31(12), 1069-1072.
12. Schouten S, Hopmans EC, Sinninghe Damste JS. The effect of maturity and depositional redox conditions on archaeal tetraether lipid palaeothermometry. *Organic Geochemistry*. 2004; 35(5), 567-571.
13. Tierney JE. Biomarker-Based Interferences of Past Climate: The TEX₈₆ Paleotemperature Proxy. *Treatise on Geochemistry (Second Edition)*. 2014; 12, 379-393).
14. Tierney JE. GDGT Thermometry: Lipid Tools for Reconstructing Paleotemperatures. *The Paleontological Society Papers*. 2012; 18, 115-131.
15. Tierney JE, Tingley MP. A TEX₈₆ surface sediment database and extended Bayesian calibration. *Scientific Data*. 2015; 2, 1-10.
16. Van Helmond NA, Sluijs A, Reichert GJ, Sinninghe Damste JS, Slomp CP, Brinkhuis H. A perturbed hydrological cycle during Oceanic Anoxic Event 2. *Geology*. 2014; 42(2), 123-126.
17. Westermann S, Vance D, Cameron V, Archer C, Robinson SA. Heterogeneous oxygenation states in the Atlantic and Tethys oceans during Oceanic Anoxic Event 2. *Earth and Planetary Science Letters*. 2014; 404(1), 178-189.